Low-Temperature Matrix Isolation and Photolysis of BCl_2N_3: Spectroscopic Identification of the Photolysis Product ClBNCl

Lisa A. Johnson, Samantha A. Sturgis, Ismail A. Al-Jihad, Bing Liu, and Julanna V. Gilbert*

Department of Chemistry and Biochemistry, University of Denver, 2190 E. Iliff Ave., Denver, Colorado 80208-2436

Received: September 10, 1998; In Final Form: November 25, 1998

BCl_2N_3 was isolated in a low-temperature argon matrix, and its FTIR spectrum was measured. Ab initio calculations were carried out to support the identification of the IR spectrum, and splitting due to the natural abundances of ^{10}B and ^{11}B was observed. The experimental infrared frequencies and assignments are as follows: 2170 cm^{-1}, the N_3 asymmetric stretch; 1350 cm^{-1}, the BN stretch; 1053 cm^{-1}, the N_3 symmetric stretch; 968 cm^{-1}, the BCl stretch. Upon UV photolysis, the BCl_2N_3 peaks decreased and new peaks at 2034 and 2087 cm^{-1} with relative integrated intensities of 4:1 appeared. Ab initio calculations were carried out and support the assignment of these features to the BN stretches in the ^{10}B and ^{11}B isotopomers of ClBNCl. This intermediate is consistent with the photolytic intermediate generated during the photolysis of $B(N_3)_3$, and the photolytic mechanism is discussed.

Introduction

Recent work in our laboratory has been concerned with the photolysis of group III−azide molecules in low-temperature inert gas matrixes.[1] These studies are motivated by the fact that several of these molecules have been shown to be precursors of group III−nitride films.[2,3] The ultimate goal of our work is to identify the intermediates generated during the photolytic decomposition and thereby gain fundamental information regarding film formation.

The first group III−azide molecule reported was $B(N_3)_3$, which undergoes a spontaneous gas-phase decomposition at room temperature to produce BN films.[1,2] The films were hexagonal when the decomposition proceeded at room temperature, and a combination of hexagonal and cubic crystal structures was produced when the $B(N_3)_3$ was allowed to decompose with mild heating or upon UV photolysis The matrix isolation studies showed that the linear molecule NNBN was generated upon broad-band UV photolysis of $B(N_3)_3$. On the basis of the usual photolytic path by which other covalent azides decompose,[4−6] the initially formed fragment would be the trigonal fragment, BN_3. The photolysis work showed, however, that if the trigonal BN_3 is formed during the photolysis, it rearranges to the linear NNBN.

It is of interest to probe the photolysis mechanisms of other trivalent group III−azide molecules. To the extent that similar molecules have analogous decomposition mechanisms, the results from low-temperature photolysis studies of $B(N_3)_3$ suggest that, for these other systems, linear intermediates may be generated upon photolysis of the parents. $B(N_3)_3$ is synthesized in the gas phase by reacting HN_3 with BCl_3 in a 3 to 1 ratio. The work done in our lab shows that $BCl_2(N_3)$ and $BCl(N_3)_2$ can be generated and isolated in a low-temperature matrix by adjusting the HN_3/BCl_3 ratio to 1:1 and 2:1, respectively. This paper reports the low-temperature matrix isolation, IR spectrum, and photolysis results for the first of these, BCl_2N_3.

In addition to being an interesting case for comparison to the $B(N_3)_3$ system, BCl_2N_3 as a monomer has not been previously isolated. Evidence of BCl_2N_3 was observed in the gas-phase study of $B(N_3)_3$ when the B−Cl stretching region was monitored as a function of the HN_3/BCl_3 reagent ratio.[2] A peak in the B−Cl stretching region of the IR spectrum was reported at 975 cm^{-1} for a HN_3/BCl_3 ratio of 1.4:1 that disappeared when the ratio was increased to 3:1.

In an early study, BCl_2N_3 was synthesized from ClN_3 and BCl_3, and its infrared and Raman spectrum were reported.[7] These data indicated that the compound exists as the trimer, $(BCl_2N_2)_3$, with an alternating BN ring in which each boron atom is bonded to two chlorine atoms and each N atom is bonded to a N_2 group. In a later study, the crystal structure of BCl_2N_3 was obtained and confirmed the trimeric ring structure.[8] The data presented here show that the species isolated in the low-temperature argon matrix is the monomeric BCl_2N_3. UV photolysis of the $BCl(N_3)_2$/Ar matrix produced the new species, ClBNCl, a compound that is isoelectronic with dichloroacetylene.

Experimental Section

BCl_2N_3 is prepared at room temperature in the gas phase by mixing BCl_3 and HN_3 in a 1:1 ratio. The HN_3 was synthesized via the NaN_3 plus excess steric acid reaction,[9] and the BCl_3 was obtained from Matheson. It is noted here that HN_3 is an explosive and toxic substance and must be synthesized and handled with care. The same apparatus that was described previously[1] for the synthesis and deposition of $B(N_3)_3$ in low-temperature argon matrixes was used for these experiments to generate low-temperature argon matrixes containing BCl_2N_3. This apparatus consists of a gas-handling manifold coupled to a RMC model 22 cryostat. In the gas-handling manifold, 1% mixtures of BCl_3/Ar and of HN_3/Ar were combined with a larger than 1:1 flow ratio of BCl_3/NH_3 and passed through a 5 L Pyrex mixing bulb, providing a 10 min reaction time and good yields of BCl_2N_3. Excess BCl_3 was used to ensure that HN_3 would be the limiting reagent and thereby avoid $BCl(N_3)_2$ or $B(N_3)_3$ production. The pressure in the synthesis manifold was controlled by throttling down an on/off valve on the manifold

10.1021/jp9836574 CCC: $18.00
Published on Web 01/26/1999

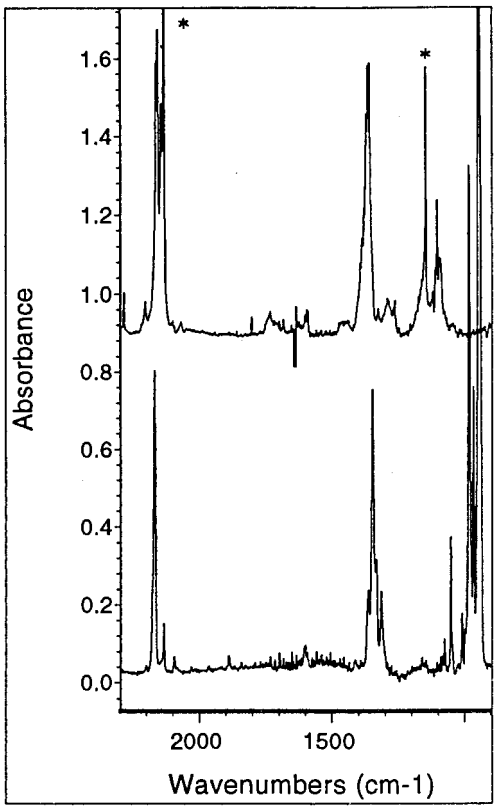

Figure 1. The bottom curve is the IR spectrum of a low-temperature argon matrix prepared with a HN_3/BCl_3 flow ratio less than 1:1. Unreacted BCl_3 is apparent by the large (off scale) peaks at 945 and 987 cm^{-1}. The top curve is the IR spectrum of $B(N_3)_3$ in a low-temperature argon matrix prepared with a HN_3/BCl_3 of greater than 3:1. The peaks indicated (*) in the top curve at 2136 and 1146 cm^{-1} are from the excess HN_3.

vacuum pump attached down stream of the 5 L mixing bulb. A metering valve was also located down stream of the mixing bulb to allow a small percentage of the gas mixture to be admitted to the cold head for deposition. It was necessary to passivate the entire synthesis manifold with pure BCl_3 prior to carrying out the synthesis if the system had been exposed to air, and for this purpose, a stainless steel gas bottle of pure BCl_3 (gas, 400 Torr) was also attached to the manifold. Gas flows were monitored with Tylan 10 sccm flowmeters, and the pressure in the gas-handling manifold was measured with a 0−10 Torr Baratron gauge (MKS).

In a typical experiment, the system was passivated, if necessary, with a few Torr of pure BCl_3 as previously described and then pumped out, and the synthesis was started by setting the flows of the reagent gases. The pressure in the manifold was set between 5 and 10 Torr, and the stainless steel metering valve on the cryostat was opened to admit a small flow of the product mixture for deposition on the cold (10 K) KCl window mounted in the cryostat. The cold head was positioned in the sample chamber of the Nicolet 5DXPC FTIR spectrometer (resolution ±2 cm^{-1}) so that the IR beam passed through the cold KCl window. A typical deposition was carried out for about 1 h, after which the matrix was photolyzed with the loosely focused output of a D_2 lamp. The progress of the deposition and of the photolysis was monitored via the IR spectrum.

Calculations were performed with Gaussian 94 on either an IBM model 250 RS6000 or a Silicon Graphics Octane work station.[10]

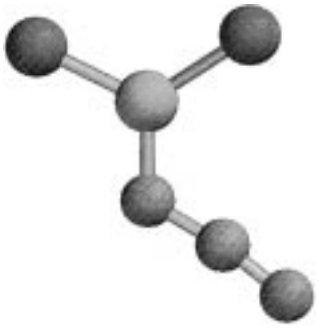

Figure 2. Calculated structure of BCl_2N_3.

TABLE 1: Optimized Geometry for BCl_2N_3

parameter	MP2/6-31G(d) (bond lengths in Å, angles in deg)
B−N	1.4312
$N_\alpha-N_\beta$	1.2420
$N_\beta-N_\gamma$	1.1664
$B-Cl_\alpha$	1.7386
$B-Cl_\beta$	1.7500
Cl−B−Cl angle	120.9
$N-B-Cl_\alpha$ angle	116.9
$N-B-Cl_\beta$ angle	122.2
$B-N_\alpha-N_\beta$ angle	121.6
$N_\alpha-N_\beta-N_\gamma$	172.6

Results and Discussion

Infrared Spectrum of BCl_2N_3. Figure 1 shows the FTIR spectrum of the matrix obtained for these studies (bottom spectrum) with a BCl_3/HN_3 flow ratio that was higher than 1:1. Unreacted BCl_3 is evident in by the appearance of peaks at 945 and 987 cm^{-1} for the ^{11}B and ^{10}B isotopomers of BCl_3, respectively.[11] The spectrum of a $B(N_3)_3$/Ar matrix (top curve) prepared with excess HN_3 is included in Figure 1 for comparison (HN_3 peaks at 2136 and 1146 cm^{-1}). The two spectra are similar in general appearance, displaying strong absorbances in the N_3 asymmetric stretching region, the BN stretching region, and the N_3 symmetric stretching region. A peak between the BCl_3 features in the bottom spectrum is observed that does not have a counterpart in the $B(N_3)_3$ spectrum.

With the flow ratio used in this experiment, it was anticipated that the product of the reaction would be BCl_2N_3. This molecule had been previously reported as the trimer, $(BCl_2N_3)_3$.[7,8] The IR spectrum reported for the trimer, however, is very different from the spectrum obtained in these experiments, and it is clear that the trimer was not deposited in the argon matrix in these experiments. To support the assignment of these features to BCl_2N_3, ab initio calculations were carried out with Gaussian 94.[10,12] The results of the geometry optimization of BCl_2N_3 for the ^{10}B and ^{11}B isotopomers at the MP2 level of theory with the 6-31G(d) basis set are included in Table 1. The calculated structure, shown in Figure 2, predicts that the molecule is nearly planar, with the terminal N_2 bent slightly (<0.05°) out of the plane. Because of the orientation of the N_3 group, the two N−B−Cl angles are not equivalent and the geometry about the boron atom is not precisely trigonal. The calculated and experimentally observed frequencies are included in Table 2 for comparison. There is a difference of a few percentage points between the calculated and observed frequencies, with essentially the same isotopic shift predicted by the calculation as observed in the spectrum. Good agreement between calculated and observed isotopic shifts has been shown to be a reliable tool in making vibrational assignments.

TABLE 2: Observed and Calculated Frequencies for the Observable Infrared Transitions of BCl_2N_3[a]

	ν_9 (cm^{-1}) B−Cl st	ν_{10} (cm^{-1}) N_3 s st	ν_{11} (cm^{-1}) B−N st	ν_{12} (cm^{-1}) N_3 as st
gas phase[b]	975			
Ar matrix (this work)				
$^{11}BCl_2N_3$	968	1053	1350	2170
$^{10}BCl_2N_3$	1010	1076	1367	
difference	42	23	17	
calculations [MP2/6-31G(d)]				
$^{11}BCl_2N_3$[c]	1030 (6%)	1097 (4%)	1428 (6%)	2165 (.2%)
$^{10}BCl_2N_3$ (this work)	1073	1123	1445	2165
difference	43	26	17	

[a] The percent deviation between the matrix and calculated values are indicated in parentheses following the calculated number. [b] In ref 2, only the B−Cl region was monitored as a function of the HN_3/BCl_3 ratio. This peak appeared as the ratio was varied from 0:1 to 1:1 and disappeared as the ratios were increased. [c] Reference 12.

The 2025−2250 cm^{-1}, 1225−1450 cm^{-1}, and 925−1150 cm^{-1} regions of the spectrum of Figure 1 are expanded and shown in parts A−C of Figure 3, respectively. The Figure 3A spectrum displays a strong peak at 2170 cm^{-1} displaced 12 cm^{-1} to the blue of the N_3 asymmetric stretch in $B(N_3)_3$. This is very close to the 2165 cm^{-1} value predicted in the calculation for the N_3 asymmetric stretch of BCl_2N_3 and is assigned as such. (This assignment is further supported by the photolysis data discussed in the next section.)

In the BN stretching region of the spectrum (Figure 3B), peaks at 1350 and 1367 cm^{-1} have the characteristic intensity relationship expected for ^{10}B and ^{11}B isotopomers, respectively, and the separation between them (17 cm^{-1}) agrees with the calculated value. On the basis of these data and the photolysis results discussed below, the 1350 cm^{-1} feature is assigned to the BN stretch in BCl_2N_3.

Examination of the region between 925 and 1150 cm^{-1} (Figure 3C) shows the BCl_3 peaks at 945 and 987 cm^{-1} plus additional features at 968, 1010, 1053, and 1076 cm^{-1}. All of these additional peaks decayed at the same rate as the 2170 and 1350 cm^{-1} features during UV photolysis, consistent with what would be observed if these are assignable to the same molecule. The intensity ratio of the 968 cm^{-1} peak to the 1010 cm^{-1} peak is 4:1, and the separation between them is consistent with the calculated boron shift for the BCl stretch of BCl_2N_3. Therefore, these peaks are assigned as such. Visualization of this vibrational mode shows it to have significant boron atom motion, so a boron isotope effect is expected. The peaks at 1053 and 1076 cm^{-1} have the requisite 4:1 intensity ratio and a difference in frequency that is very close to that predicted by the calculations for the N_3 symmetric stretches in $^{10}BCl_2N_3$ and $^{11}BCl_2N_3$. Thus, the 1053 cm^{-1} feature is assigned as the N_3 symmetric stretch in $^{11}BCl_2N_3$ (and the 1076 cm^{-1} peak as the N_3 symmetric stretch in $^{10}BCl_2N_3$).

The chlorine isotope shifts for the BCl stretches in $B^{35}Cl^{37}ClN_3$ and $B^{37}Cl_2N_3$ relative to $B^{35}Cl_2N_3$ were calculated to be 2 and 4 cm^{-1}, respectively. These cannot be observed since the BCl spectral region is dominated by the very large BCl_3 peaks.

Photolysis of BCl_2N_3. When the BCl_2N_3/Ar matrix was irradiated with the loosely focused deuterium lamp, immediate changes in the infrared spectrum of the matrix were observed. Parts A−C of Figure 4 show the 2025−2250 cm^{-1}, 1225−1450 cm^{-1}, and 925−1150 cm^{-1} regions of the infrared spectrum as a function of photolysis time. In the 2025−2250 cm^{-1} region, the 2170 cm^{-1} peak decreases and new peaks at 2034 and 2087 cm^{-1} appear and continue to grow during the photolysis. These new peaks display a 4:1 intensity ratio suggesting that these are ^{10}B and ^{11}B isotopomers of a species containing a single boron atom. All of the peaks in the 1225−1450 cm^{-1} region and in the 925−1150 cm^{-1} region decrease with photolysis time.

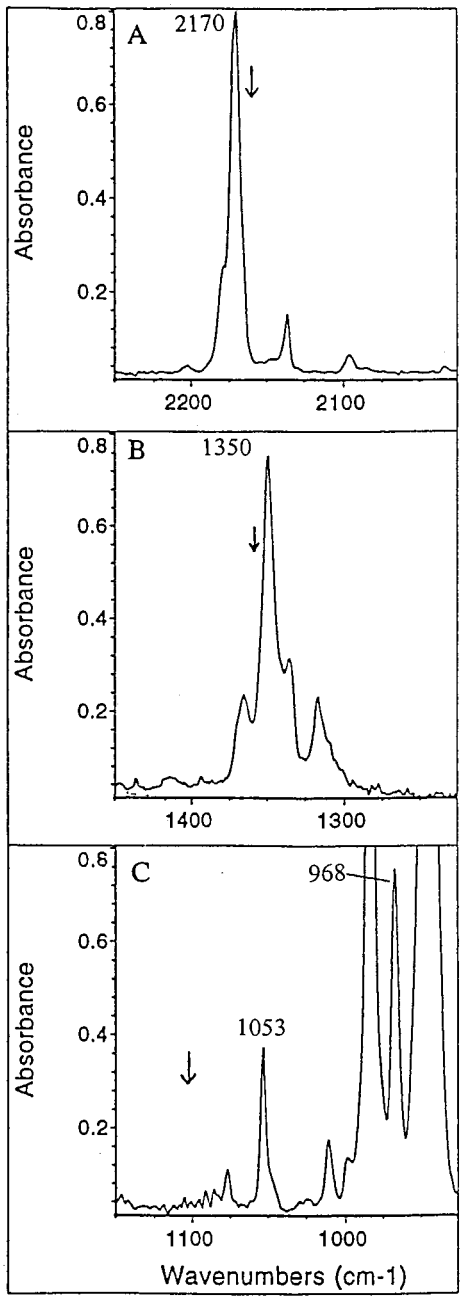

Figure 3. Expanded regions of the FTIR spectrum from Figure 1: (A) the azide asymmetric stretching region, 2025−2250 cm^{-1}; (B) the BN stretching region, 1225−1450 cm^{-1}; (C) the azide symmetric stretching region, 925−1150 cm^{-1}. The arrows indicate the positions of the $B(N_3)_3$ peaks for comparison.

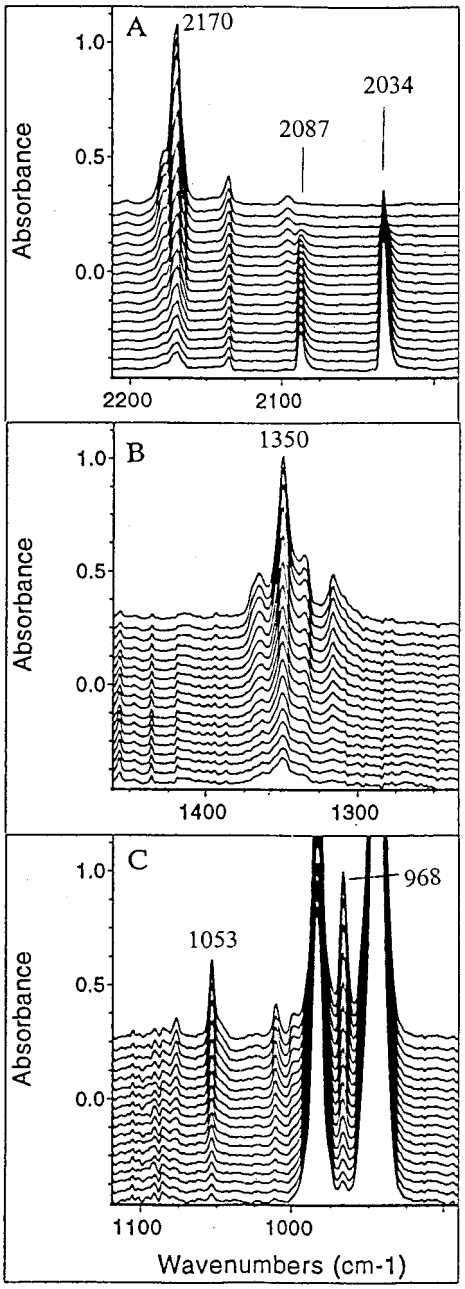

Figure 4. The same regions as shown in Figure 3 showing the changes that occur in the spectra as the BCl_2N_3 matrix was photolyzed for 2 h. Photolysis time increases from top to bottom in each. The average time intervals between the spectra are 2 min for the first three spectra, 5 min for the next eight spectra, 12 min for the next six spectra, and 26 min for the last spectrum.

Plots of normalized peak height vs photolysis time are shown in Figure 5. Clearly, all of the peaks assigned to BCl_2N_3 decay at the same rate. The two peaks that appear at 2087 and 2034 cm^{-1} display the same growth rate that is consistent with the assumption that the species associated with these peaks is a product of the BCl_2N_3 photolysis. The HN_3 peak at 2136 cm^{-1} decays at a much slower rate and so is not associated with the appearance of the product.

The photolysis of $B(N_3)_3$ in low-temperature argon matrixes generated the linear species NNBN. In those studies, it was proposed that a trigonal BN_3 fragment was formed initially, followed by rearrangement to the more stable linear structure. If BCl_2N_3 follows a similar photolytic pathway, the initial photofragment would be trigonal BCl_2N. To the extent that this

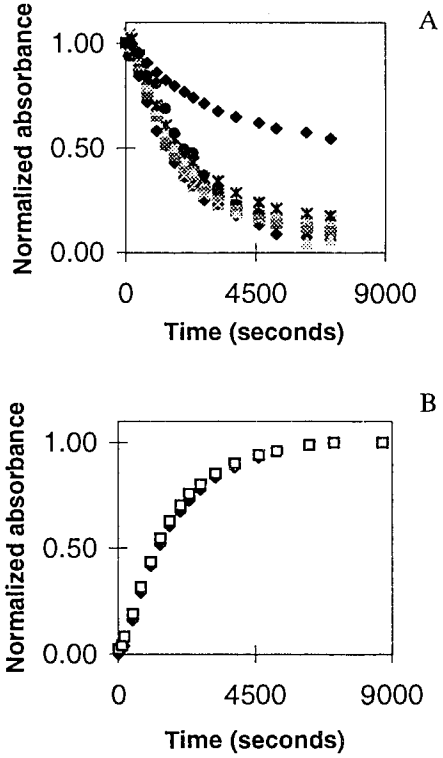

Figure 5. (A) Normalized peak heights vs photolysis time for the HN_3 peak at 2146 cm^{-1} (black diamonds) and for the BCl_2N_3 peaks at 2170, 1349, 1365, 967, 1011, 1053, and 1077 cm^{-1}. All of the BCl_2N_3 peaks are seen to decay at the same rate. (B) Normalized peak heights vs photolysis time for the two peaks at 2034 and 2087 cm^{-1}. These peaks grow in at the same rate at which the BCl_2N_3 peaks disappear.

TABLE 3: Bond Lengths in ClBNCl Obtained from the Geometry Optimization [B3PW91/6-311G*] (Molecule Was Predicted To Be Linear)

B−Cl bond length (Å)	B−N bond length (Å)	N−Cl bond length (Å)
1.6950	1.2378	1.6224

fragment is not stable, rearrangement would occur as in BN_3. Frequencies were computed for trigonal BCl_2N, linear ClBN, and the molecules ClClBN and ClBNCl, species that could form assuming no rearrangement, additional photolysis, and rearrangement to straight chain forms, respectively. The BN stretches computed for the ^{10}B and ^{11}B isotopomers of ClBNCl have the best agreement with the observed peaks at 2087 and 2034 cm^{-1}, and the optimized geometry and the calculated frequencies for this molecule are listed in Tables 3 and 4. The calculations suggest that the asymmetric BCl stretch should be observable; however, the BCl_3 peaks dominate this region of the spectrum. In matrixes prepared with a smaller BCl_3 excess such that the BCl_3 was not off scale, two things were observed: a mixture of $BCl_2(N_3)$ and $BCl(N_3)_2$ was deposited in the matrix, and upon photolysis, the BCl_3 peaks showed a small increase. Since it is very unlikely that BCl_3 could be generated via photolysis, this growth was attributed to BCl stretching modes in the photoproducts, one of which is ClBNCl. Work is in progress on the $BCl(N_3)_2$ system.

ClBNCl is isoelectronic with 1,2-dichloroacetylene and, similarly, is a linear molecule. Analogous physical and chemical behavior is expected for these two compounds.[13] Indeed, there are similarities between the IR spectra of these two molecules, although, unlike 1,2-dichloroacetylene, stretches involving the central bond are IR active in ClBNCl. ClCCCl reacts spontaneously with O_2 (to form phosgene), so ClBNCl is likewise predicted to be unstable in the presence of O_2.

TABLE 4: Comparison of the Observed and Calculated [B3PW91/6-311G*] Infrared Frequencies in ClBNCl[a,b]

	ν_1 (cm^{-1}) B−N st	ν_2 (cm^{-1}) Cl−BN−Cl sym st	ν_3 (cm^{-1}) Cl−BN−Cl as st
Ar matrix (this work)			
$Cl^{11}BNCl$	2034	not observed	∼945
$Cl^{10}BNCl$	2087		
difference	53		
calculations [B3PW91/6-311G*]			
$Cl^{11}BNC$	2089 (345)	458 (4)	962 (44)
$Cl^{10}BNCl$	2146		977
difference	57		15

[a] The Calculated Intensities in km/mol are included in parentheses after the calculated frequencies. [b] Three additional infrared active modes for $^{10}BCl_2N_3$ ($^{11}BCl_2N_3$) were calculated at 313 (325), 311 (323), and 105 (105) cm^{-1}. [c] BCl_3 features completely dominate this region of the spectrum, but evidence has been observed to indicate that the Cl−BN−Cl asymmetric stretch appears near the 945 cm^{-1} BCl_3 peak.

Conclusions

This study is part of the investigation of the $BCl_3 + nHN_3$ ($n = 1, 2, 3$) reaction system that is ongoing in our lab. In the first part of this work, $B(N_3)_3$ was isolated and photolyzed in a low-temperature argon matrix.[1] In the work reported here, monomeric BCl_2N_3 was isolated and photolyzed in a low-temperature argon matrix. In both studies, insight into the photolysis mechanisms was obtained.

In several respects, BCl_2N_3 and $B(N_3)_3$ are similar. Both molecules are sufficiently stable in the gas phase to pass through a Pyrex/stainless steel/Teflon gas manifold and a stainless steel metering valve and be deposited in a low-temperature argon matrix. Both molecules undergo photolysis to generate linear 4-atom intermediate products. The process by which the linear structures are formed is of fundamental interest and is being studied. Self-assembly of the NNBN photointermediates has been proposed as the mechanism by which the BN films are produced in the $B(N_3)_3$ system,[14] and this mechanism is being investigated computationally.[15] Studies of BCl_2N_3 photodecomposition in the gas phase have not been carried out but would be of interest. One can imagine self-assembly of three ClBNCl molecules to generate hexachloroborazine, a molecule that is known to exist.[16]

Continuing work on these interesting systems is proceeding in our lab. $BCl(N_3)_2$ has proved to be the most elusive of the three boron azide molecules but has just recently been successfully isolated in a low-temperature matrix, and photolysis studies have begun. LIF studies of the electronic states of the intermediates NNBN and ClBNCl are planned, and work on analogous aluminum systems is in progress.

Acknowledgment. This work was supported by the National Science Foundation under Grant CHE-9527080 and by the Research Corporation under Grant GG0037.

References and Notes

(1) Al-Jihad, I. A.; Liu, B.; Linnen, C. J.; Gilbert, J. V. *J. Phys. Chem.* **1998**, *102*, 6220.

(2) Mulinax, R. L.; Okin, G. S.; Coombe, R. D. *J. Phys. Chem.* **1995**, *99*, 6294.

(3) Linnen, C. J.; Macks, D. E.; Coombe, R. D. *J. Phys. Chem.* **1997**, *101*, 1602.

(4) Patel, D.; Pritt, A. T., Jr.; Benard, D. J. *J. Phys. Chem.* **1986**, *90*, 1931.

(5) MacDonald, M. A.; David, S. J.; Coombe, R. D. *J. Chem. Phys.* **1986**, *84*, 5513.

(6) Coombe, R. D.; Patel, D.; Pritt, A. T., Jr.; Wodarczk, F. J. *J. Chem. Phys.* **1981**, *75*, 2177.

(7) Paetzold, P. I.; Gayoso, M.; Dehnicke, K. *Z. Chem. Ber.* **1965**, *98*, 1173.

(8) Mueller, U. *Z. Anorg. Allg. Chem.* **1971**, *382*, 110.

(9) Schlie, L. A.; Wright, M. W. *J. Chem. Phys.* **1990**, *92*, 394.

(10) Frisch, M. J.; Trucks, G. W.; Schlegel, H. B.; Gill, M. W.; Johnson, B. G.; Robb, M. A.; Cheeseman, J. R.; Keith, T. A.; Petersson, G. A.; Montgomery, J. A.; Raghavachari, K.; Al-Laham, M. A.; Zakrzewski, V. G.; Ortiz, J. V.; Foresman, J. B.; Cioslowski, J.; Stefanov, B. B.; Nanayakkara, A.; Challacombe, M.; Peng, C. Y.; Ayala, P. Y.; Chen, W.; Wong, M. W.; Andres, J. L.; Replogle, E. S.; Gomperts, R.; Martin, R. L.; Fox, D. J.; Binkley, J. S.; Defrees, D. J.; Baker, J.; Stewart, J. P.; Head-Gordon, M.; Gonzalez, C.; Pople, J. A. *Gaussian 94*, revision A.1; Gaussian, Inc.: Pittsburgh, PA, 1995.

(11) Scruby, R. E.; Lacher, J. R.; Park, J. D. *J. Chem Phys.* **1951**, *19*, 386.

(12) Geometry optimization and frequencies were originally performed by G. S. Okin and R. D. Coombe with Gaussian 92 on the ^{11}B isotopomer and repeated for this work with Gaussian 94 for both the ^{11}B and the ^{10}B isotopomers.

(13) Klaboe, P.; Klotser-Jensen, E.; Christensen, D. H.; Johnsen, I. *Spectrochim. Acta* **1970**, *26A*, 1567.

(14) Coombe, R. D. Private communication, 1998.

(15) Hobbs, K.; Coombe, R. D. Manuscript in preparation.

(16) Paetzold P. I. *Z. Anorg. Allg. Chem.* **1963**, 326, 47, 53, 58, 64.